

REGULAR PAPER

Orientation control of two-dimensional perovskite
 $(\text{CH}_3(\text{CH}_2)_3\text{NH}_3)_2(\text{CH}_3\text{NH}_3)_{n-1}\text{Pb}_n\text{I}_{3n+1}$ ($n = 2$)
thin films by thermal annealing

To cite this article: Yuya Futamura *et al* 2023 *Jpn. J. Appl. Phys.* **62** SK1007

View the [article online](#) for updates and enhancements.

You may also like

- [THE ROLE OF METHANOL IN THE CRYSTALLIZATION OF TITAN'S PRIMORDIAL OCEAN](#)
Frédéric Deschamps, Olivier Mouis, Carmen Sanchez-Valle et al.
- [Raman spectroscopy in layered hybrid organic-inorganic metal halide perovskites](#)
Davide Spirito, Yaiza Asensio, Luis E Hueso et al.
- [Structural stability and optoelectronic properties of tetragonal MAPbI₃ under strain](#)
Lei Guo, Gao Xu, Gang Tang et al.



Orientation control of two-dimensional perovskite $(\text{CH}_3(\text{CH}_2)_3\text{NH}_3)_2(\text{CH}_3\text{NH}_3)_{n-1}\text{Pb}_n\text{I}_{3n+1}$ ($n = 2$) thin films by thermal annealing

Yuya Futamura, Fumiya Sano, Haruki Yasuda, Shoichiro Hino, Yasushi Sobajima, and Norimitsu Yoshida*

Gifu University, Yanagido 1-1, Gifu 501-1193, Japan

*E-mail: yoshida.norimitsu.v0@f.gifu-u.ac.jp

Received December 26, 2022; revised February 3, 2023; accepted February 19, 2023; published online March 27, 2023

It has been attempted to preferentially orientate Pb-I layers in two-dimensional (2D) organic-inorganic hybrid perovskite thin films $(\text{CH}_3(\text{CH}_2)_3\text{NH}_3)_2(\text{CH}_3\text{NH}_3)\text{Pb}_2\text{I}_7$ perpendicular to substrates only by thermal annealing after spin coating of a reagent solution for improvements in the energy-conversion-efficiency of solar cells. It is found from X-ray diffraction measurements that the ratio of diffraction intensity from the (202) plane to that from the (060) plane becomes larger in thermally annealed (50 °C–135 °C) samples. This indicates that the Pb-I layer tends to grow perpendicular to the surface of the substrate. In particular, the ratio has reached 8.2, which is larger compared with the ratio of 2.7 for the randomly oriented powder sample, for the sample prepared on SnO_2 substrates. Such (202) oriented films seem to contribute to improvements in the energy-conversion-efficiency of tandem-type solar cells utilizing the 2D perovskite thin films as an active layer of the top cell.

© 2023 The Japan Society of Applied Physics

1. Introduction

Organic–inorganic hybrid perovskite such as $\text{CH}_3\text{NH}_3\text{PbI}_3$ is one of the promising materials for next-generation solar cell materials.^{1–4} The highest energy-conversion-efficiency solar cells utilizing perovskite materials as an active layer that has been reached is 25.7%^{3,5} and will be improved furthermore. However, dissolution and degradation of the materials by moisture and oxygen are the most serious problems^{6,7} for realizing solar cells with longer lifetimes.

Quasi two-dimensional (2D) perovskites have attracted much attention as one of the candidates for alternative solar cell materials.^{8–30} The material has better hydrophobicity compared with that of $\text{CH}_3\text{NH}_3\text{PbI}_3$ due to the existence of alkyl chains such as $\text{CH}_3(\text{CH}_2)_3-$ and thus is more stable against moisture. One of the helpful utilizations of the 2D perovskite materials is passivation of the surface of three-dimensional perovskite such as $\text{CH}_3\text{NH}_3\text{PbI}_3$.¹⁸ On the other hand, 2D perovskite has also been applied to the active layers of solar cells.^{19–22} For example, Ruddlesden–Popper 2D $(\text{CH}_3(\text{CH}_2)_3\text{NH}_3)_2(\text{CH}_3\text{NH}_3)_{n-1}\text{Pb}_n\text{I}_{3n+1}$ films have been tried to apply to an active layer due to having the bandgap energies ranged from 1.7 eV to 2.3 eV by modifying the number of Pb–I layers n ($n = 1 \sim 4$).^{19–22}

It is known that the inorganic Pb–I layer grows perpendicular to the surface of the substrate for the film of $n \geq 3$. This orientation of the Pb–I layer is useful for the active layer in solar cells because photoexcited carriers transport in such layers to the direction of the thickness.^{19–29} For $n \leq 2$ materials, however, the layer is known to grow parallel to the surface of the substrate.¹⁹ In this case, organic cation spacers between the layers inhibit the carrier transport in solar cells.^{19–29} Thus, orientation control^{23–29} of the Pb–I layer in 2D perovskites for $n \leq 2$ seems to be important for the application of these materials to solar cells. Furthermore, the bandgap energy is known to be larger (2.3 eV for $n = 1$ and 2.1 eV for $n = 2$).¹⁹ Thus, these materials can be used as an active layer for the top cell of tandem-type solar cells.

It has been reported by some authors that the orientation of the Pb–I layer can be controlled by modifying some preparation conditions of the film, for example, the kind of solvent,²³ rotation speed^{24,25} and isomeric reagents.²⁶

Among them, there are some papers for the orientation control of the layer for the $n = 1$ material.^{24,25} However, there are few papers trying the orientation control of the Pb–I layers for the $n = 2$ material $(\text{CH}_3(\text{CH}_2)_3\text{NH}_3)_2(\text{CH}_3\text{NH}_3)\text{Pb}_2\text{I}_7$. Hereafter, $\text{CH}_3(\text{CH}_2)_3\text{NH}_3$ and CH_3NH_3 are abbreviated as BA and MA, respectively. That is, $(\text{CH}_3(\text{CH}_2)_3\text{NH}_3)_2(\text{CH}_3\text{NH}_3)\text{Pb}_2\text{I}_7$ is expressed as $(\text{BA})_2(\text{MA})\text{Pb}_2\text{I}_7$.

In this study, therefore, we have tried to prepare $(\text{BA})_2(\text{MA})\text{Pb}_2\text{I}_7$ thin films having the perpendicular orientation of the Pb–I layers to the substrate only by thermal annealing after spin coating of reagent solution. To the authors' knowledge, this study is the first to do this.

2. Experimental methods

$(\text{BA})_2(\text{MA})\text{Pb}_2\text{I}_7$ thin films were prepared by a spin coating method. Lead iodide (PbI_2), normal butylamine hydroiodide ($n\text{-C}_4\text{H}_{11}\text{NHI}$) and methylamine hydroiodide (CH_5NHI) were used as reagents unless otherwise stated and N, N-dimethylformamide ($\text{C}_3\text{H}_7\text{NO}$: DMF) was employed as a solvent. Note that iso butylamine hydroiodide ($\text{iso-C}_4\text{H}_{11}\text{NHI}$)²⁶ was also employed as a reagent. The solutions with concentrations from 0.3 M to 1.5 M were stirred at 80 °C for 30 min and then naturally cooled to RT. The concentration of the solution was defined, for example for the case of 1 M, as the ratio $\text{PbI}_2 : \text{C}_4\text{H}_{11}\text{NHI} : \text{CH}_5\text{NHI} = 1 \text{ mmol} : 1 \text{ mmol} : 0.5 \text{ mmol}$ to 1 ml of DMF.³⁰

Quartz glasses with dimensions of 2 cm × 2 cm and a thickness of 0.5 mm were employed as substrates. For implementing 2D perovskite $(\text{BA})_2(\text{MA})\text{Pb}_2\text{I}_7$ films in solar cells, it seems to be important to investigate the trend of the crystalline orientation of the material deposited on functional materials, that is, the electron transport material (an n-type semiconductor). It is known that SnO_2 is one of the candidates for the electron transport material in perovskite solar cells.³¹ In this study, commercially available type-VU by AGC Inc. was tentatively employed as a SnO_2 substrate. The thickness of the substrate was 0.9 mm and the dimension was fixed at 2 cm × 2 cm. For the cleaning of these substrates, they were immersed in an organic solvent (Semico Clean 56) for 10 min and then ultrasonically treated in ethanol for 10 min. Further, these substrates were irradiated with ultraviolet light for 15 min and were heated to 115 °C in advance before

deposition of the film. Then, 100 ml of the solution was dropped onto a substrate and spin-coated at 6000 rpm for 30 s. After the spin coating, the samples were immediately annealed for 5 min on a hot plate in air. The annealing temperature was varied from RT to 150 °C. All these processes were performed in air with a humidity less than 35%.

The thickness of deposited films was estimated by observations of cross-sectional views of the film using a scanning electron microscope (Hitachi S-4800). It is found that the thickness ranges from 0.1 μm to 0.6 μm for almost all the films. Except for those films, the thickness is found to range from 1.1 μm to 1.8 μm prepared by spin coating the solution with concentrations of 1.0 M and 1.5 M on the SnO₂ substrate and annealed at 50 °C or higher.

The X-ray diffraction (XRD) patterns of the sample were measured (Rigaku SmartLab) by θ - 2θ method using the CuK α line for analyzing the structure and orientation of the film. The acceleration voltage and current for the Cu target were fixed at 45 kV and 200 mA, respectively. The resolution of the diffraction angle was set at 0.01°. The measurement was performed from $2\theta = 2^\circ$ to $2\theta = 40^\circ$ with a scan speed of 3° min^{-1} .

Figure 1 shows a schematic illustration of the crystal structure for (BA)₂(MA)Pb₂I₇ and its (020) planes^{19,30} for an example of (0*k*0) planes. When diffraction peaks from (0*k*0) planes are preferentially observed, the Pb–I layer grows parallel to the surface of the substrate as shown in this figure.^{19,30} On the other hand, the diffraction peak from a (*h*0*l*) plane, which is perpendicular to (0*k*0) planes because this material possesses an orthorhombic system,^{19,30} becomes larger when the Pb–I layer tends to grow perpendicular to the surface of the substrate. Thus, we evaluated the orientation degree of the (202) plane (not shown in Fig. 1) in this 2D perovskite thin film by defining the intensity ratio *r* as

$$r = \frac{I_{(202)}}{I_{(060)}}, \quad (1)$$

in which *I*₍₂₀₂₎ and *I*₍₀₆₀₎ indicate integral intensities of the diffraction peak from the (202) plane ($2\theta = 28.3^\circ$) and (060) plane ($2\theta = 13.5^\circ$),^{19,30} respectively. Note that the intensity of the diffraction peak from the (060) plane is the largest in (0*k*0) planes for our XRD data so this peak seems to be appropriate for a reference to the peak from the (202) plane for evaluating the intensity ratio *r*. Also, note that the size of the crystalline grain was estimated from Scherrer's formula using full width at half maximum of diffraction peaks.

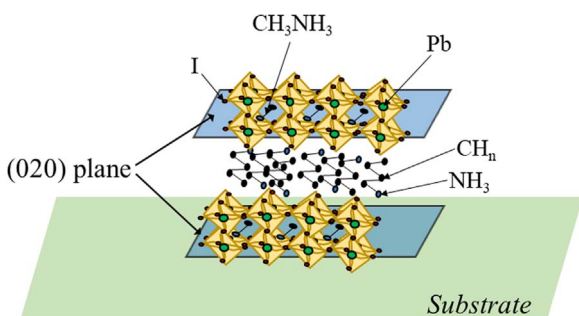


Fig. 1. (Color online) A schematic illustration of the crystal structure of (BA)₂(MA)Pb₂I₇¹⁹ (020) planes is indicated as a guide for the eyes. Species constructing the material are also indicated.

3. Results and discussion

3.1. X-ray diffraction patterns of 2D perovskite (BA)₂(MA)Pb₂I₇ films

Figure 2 shows XRD patterns of deposited (BA)₂(MA)Pb₂I₇ films on quartz glass substrates with solution concentrations of (a) 0.3 M, (b) 1.0 M and (c) 1.5 M for various annealing temperatures as indicated in the figure. It is found that the diffraction peaks from (0*k*0) planes of (BA)₂(MA)Pb₂I₇ are observed for all data. It is also found that little diffraction peaks from the (202) plane at $2\theta = 28.3^\circ$ are observed for samples annealed at RT. This indicates that the Pb–I layer in (BA)₂(MA)Pb₂I₇ films annealed at RT after spin coating of the solution grows parallel to the surface of the substrate, which is the same result as that in Ref. 13. For such films, the intensity ratios *r* are less than 1 (see Fig. 4).

On the other hand, the diffraction peaks from the (202) plane can be observed for samples annealed at 50 °C or higher after spin coating of the solution. The ratio *r* becomes roughly in the range 1–2 in some films annealed at 50 °C or higher after spin coating of the solution with the concentration of 1.0 M [see Fig. 2 (b)] and a film annealed at 100 °C with the concentration of 1.5 M [see Fig. 2 (c)]. In such films, the Pb–I layer slightly tends to grow perpendicular to the surface of the substrate.

Figure 3 shows XRD patterns of (BA)₂(MA)Pb₂I₇ films on SnO₂ substrates with solution concentrations of (a) 0.3 M, (b) 1.0 M and (c) 1.5 M for various annealing temperatures as indicated in the figure. It is found that the diffraction peaks

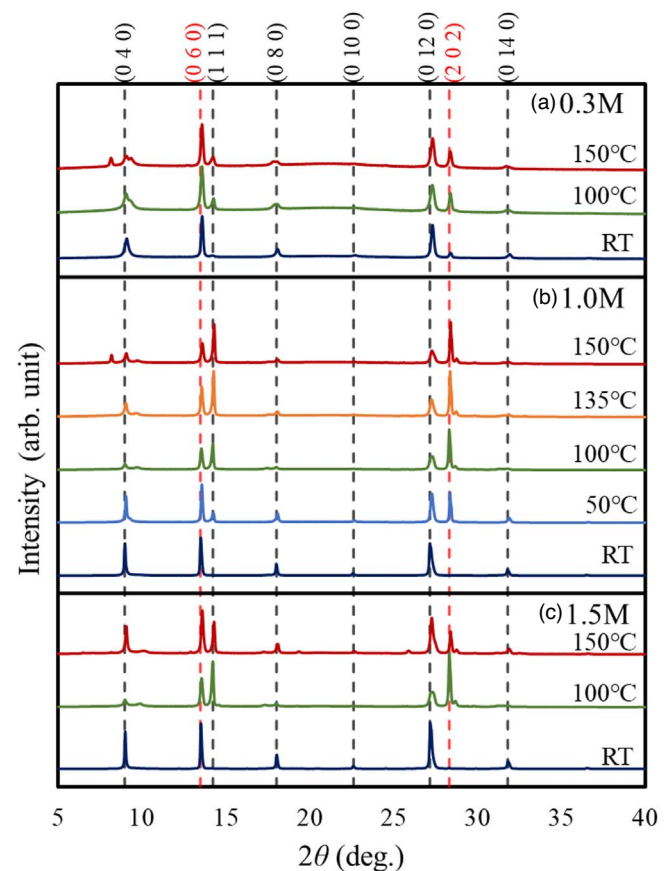


Fig. 2. (Color online) XRD patterns of (BA)₂(MA)Pb₂I₇ films deposited on quartz glasses annealed at various temperatures after the spin coating of the solution with concentrations of (a) 0.3 M, (b) 1.0 M and (c) 1.5 M. The plane indices and annealing temperatures are also indicated.

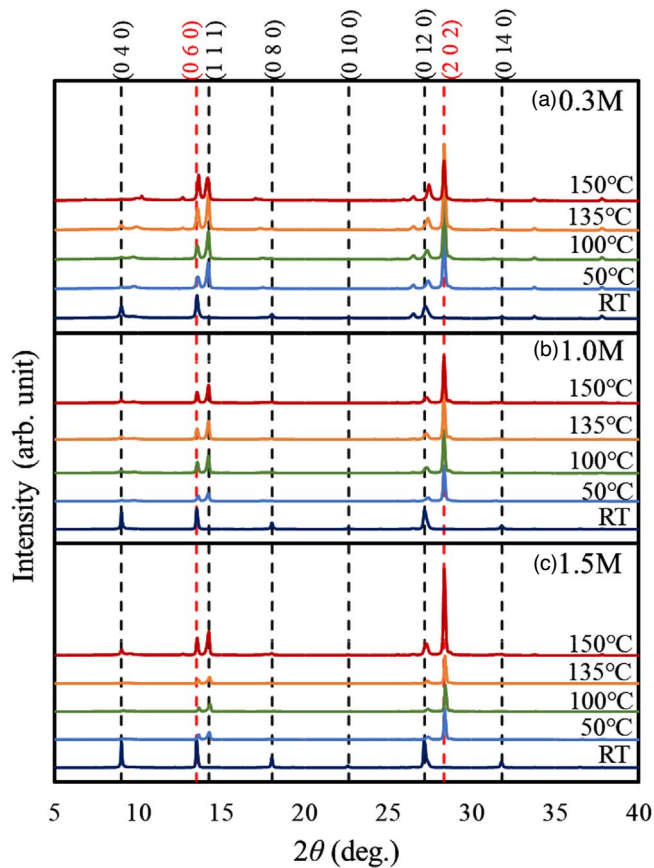


Fig. 3. (Color online) XRD patterns of $(\text{BA})_2(\text{MA})\text{Pb}_2\text{I}_7$ films deposited on SnO_2 substrates annealed at various temperatures after the spin coating of the solution with concentrations of (a) 0.3 M, (b) 1.0 M and (c) 1.5 M. The plane indices and annealing temperatures are also indicated.

from $(0k0)$ planes of $(\text{BA})_2(\text{MA})\text{Pb}_2\text{I}_7$ are observed for all data and that little diffraction peaks from the (202) plane at $2\theta = 28.3^\circ$ are observed for samples annealed at RT. This indicates that the Pb–I layer in $(\text{BA})_2(\text{MA})\text{Pb}_2\text{I}_7$ films annealed at RT after spin coating of the solution grows parallel to the surface of the substrate and the intensity ratios $r = I_{(202)}/I_{(060)}$ are less than 1 (see Fig. 4). These results are almost the same¹⁹⁾ as those for films deposited on quartz glass substrates shown in Fig. 2.

However, the diffraction peaks from the (202) plane can be observed for all samples annealed after spin coating of the solution. Further, the ratio r becomes larger than 3 for almost all the samples except for one annealed at 135°C after spin coating of the solution with a concentration of 0.3 M (see Fig. 4). Note that the ratio r for randomly oriented powder is 2.7³⁰⁾ (see a dashed line in Fig. 4). Accordingly, we can conclude that the film has preferentially (202) oriented on SnO_2 . In other words, the Pb–I layer on SnO_2 is oriented perpendicular to the surface of the substrate in thermally annealed $(\text{BA})_2(\text{MA})\text{Pb}_2\text{I}_7$ films.

It is noted that the grain size of the film seems to be independent of the annealing temperature. That is, the grain sizes for (060) and (202) planes are roughly 50 ± 10 nm and 60 ± 10 nm, respectively.

Figure 4 summarizes the intensity ratio r defined as Eq. (1) in 2D perovskite $(\text{BA})_2(\text{MA})\text{Pb}_2\text{I}_7$ thin films deposited on glass (open circles) and SnO_2 substrates (closed circles) as a function of annealing temperature. It is found that the

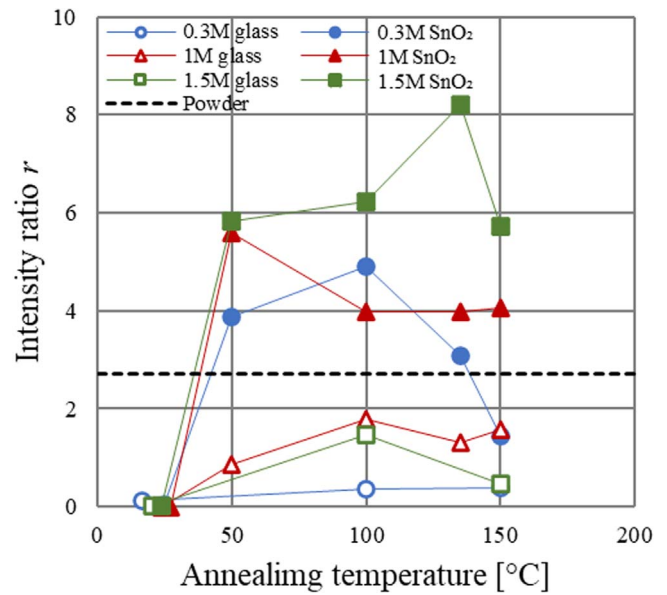


Fig. 4. (Color online) The intensity ratio r of the $(\text{BA})_2(\text{MA})\text{Pb}_2\text{I}_7$ films deposited on quartz glasses (closed symbols) and SnO_2 substrates (open symbols) as a function of the annealed temperature. Blue circles, red triangles and green squares indicate data for the film prepared using the solution with concentrations 0.3 M, 1.0 M and 1.5 M, respectively. The ratio $r = 2.7$ for randomly oriented powder¹⁴⁾ is also indicated by a dashed line.

intensity ratio r becomes larger when the sample is thermally annealed after spin coating compared with those of samples kept at RT. Such a trend is observed for all samples prepared from each concentration of the solution. It is also found that the ratio r is larger for samples deposited on SnO_2 compared with those on quartz glass. In the former substrate, the ratio r reaches to 8.2 for a film annealed at 135°C after spin coating of the solution with a concentration of 1.5 M [see also Fig. 3(c)]. Note that the ratio r roughly tends to decrease for higher annealing temperatures for all samples, especially at 150°C .

It seems to be worth mentioning here that we have also tried to prepare (202) oriented $(\text{BA})_2(\text{MA})\text{Pb}_2\text{I}_7$ films using iso- $\text{C}_4\text{H}_{11}\text{NHI}$ ²⁶⁾ as one of the reagents. It has been reported that $(\text{BA})_2(\text{MA})_3\text{Pb}_4\text{I}_{13}$, which corresponds to $n = 4$ material for the $(\text{BA})_2(\text{MA})_{n-1}\text{Pb}_n\text{I}_{3n+1}$ group, can be deposited as (202) orientation.²⁶⁾ That is, iso- $\text{C}_4\text{H}_{11}\text{NHI}$ may play a role in the Pb–I layer growing perpendicular to the surface of the substrate. However, in this study, no (202) preferential orientation film was observed (not shown) for $(\text{BA})_2(\text{MA})\text{Pb}_2\text{I}_7$ films under almost the same deposition conditions described in the Sect. 2.

3.2. Crystalline orientation of $(\text{BA})_2(\text{MA})\text{Pb}_2\text{I}_7$ films

We have found in this study that Pb–I layers, which act as a current pass for electronic devices^{19–29)} such as solar cells, in $(\text{BA})_2(\text{MA})\text{Pb}_2\text{I}_7$ films can be oriented perpendicular to the surface of the substrate only by thermal annealing of the spin-coated reagent solution. We think that the interaction between the surface of the substrate and the 2D Pb–I slabs of $(\text{BA})_2(\text{MA})\text{Pb}_2\text{I}_7$ in the solution seems to be larger for the surface of the slab but not for the edge. Thus, the Pb–I layer originally tends to grow parallel to the surface of the substrate. Such films would essentially exhibit $(0k0)$ orientation as shown in our data for films annealed at RT. On the other hand, the energy of the Pb–I 2D slabs would be higher

than that at RT when the solution just spin-coated is thermally annealed. Consequently, the slab of the Pb-I layer becomes unstable and thus tends to have a perpendicular component to the surface of the substrate.

For thermally annealed films, the intensity ratio r [Eq. (1)] becomes larger for films deposited on SnO₂ substrates ($r > 3$) compared with those on quartz glass substrates ($r < 2$) as shown in Fig. 4. We guess epitaxial-like growth of (BA)₂(MA)Pb₂I₇ slab occurs at the surface of microcrystalline SnO₂ substrate.

4. Conclusions

We have tried to prepare 2D perovskite (BA)₂(MA)Pb₂I₇ films having (202) orientation for applying this material to solar cells. We have demonstrated that (BA)₂(MA)Pb₂I₇ films having (202) orientation can be prepared only by thermal annealing of the film at 50 °C–150 °C just after the spin coating of the solution. The intensity ratio r reached an 8.2 maximum. This material has a wide bandgap energy of 2.1 eV so that such perpendicularly oriented 2D perovskite films could be utilized as an active layer of top cells in tandem-type solar cells. Further experiments and simulations^{32,33} are needed to elucidate the mechanism of the crystalline orientation of 2D perovskite films.

Acknowledgments

We would like to thank Professor Fumitaka Ohashi of Gifu University for their helpful technical support of the XRD instrument.

- 1) A. Kojima, K. Teshima, Y. Shirai, and T. Miyasaka, *J. Am. Chem. Soc.* **131**, 6050 (2009).
- 2) J. Burschka, N. Pellet, S.-J. Moon, R. H.-Baker, P. Gao, M. K. Nazeeruddin, and M. Grätzel, *Nature* **499**, 316 (2013).
- 3) M. Jeong et al., *Science* **369**, 1615 (2020).
- 4) C. Chen et al., *Nature* **612**, 266 (2022).
- 5) M. A. Green, E. D. Dunlop, G. Siefert, M. Yoshita, N. Kopidakis, K. Bothe, and X. Hao, *Prog. Photovolt. Res. Appl.* **31**, 3 (2023).
- 6) A. Arakcheeva, D. Chernyshov, M. Spina, L. Forró, and E. Horváth, *Acta Cryst.* **B72**, 716 (2016).
- 7) J. Huang, S. Tan, P. D. Lund, and H. Zhou, *Energy Environ. Sci.* **10**, 2284 (2017).
- 8) J. Calabrese, N. L. Jones, R. L. Harlow, N. Herron, D. L. Thorn, and Y. Wang, *J. Am. Chem. Soc.* **113**, 2328 (1991).
- 9) D. B. Mitzi, C. A. Field, W. T. A. Harrison, and A. M. Guloy, *Nature* **369**, 467 (1994).
- 10) D. B. Mitzi, M. T. Prikas, and K. Chondroudis, *Chem. Mater.* **11**, 542 (1999).
- 11) Z. Cheng and J. Lin, *Cryst. Eng. Comm.* **12**, 2646 (2010).
- 12) L. Dou et al., *Science* **349**, 1518 (2015).
- 13) R. Hamaguchi, M. Yoshizawa-Fujita, T. Miyasaka, H. Kunugita, K. Ema, Y. Takeoka, and M. Rikukawa, *Chem. Commun.* **53**, 4366 (2017).
- 14) C. M. M. Soe et al., *J. Am. Chem. Soc.* **139**, 16297 (2017).
- 15) L. Mao, W. Ke, L. Pedesseau, Y. Wu, C. Katan, J. Even, M. R. Wasielewski, C. C. Stoumpos, and M. G. Kanatzidis, *J. Am. Chem. Soc.* **140**, 3775 (2018).
- 16) Z. Yao, Y. Zhou, X. Yin, X. Li, J. Han, M. Tai, Y. Zhou, J. Li, F. Hao, and H. Lin, *Cryst. Eng. Comm.* **20**, 6704 (2018).
- 17) C. M. M. Soe et al., *Proc. Natl. Acad. Sci. U. S. A.* **116**, 58 (2019).
- 18) E. H. Jung, N. J. Jeon, E. Y. Park, C. Su Moon, T. J. Shin, T. Y. Yang, J. H. Noh, and J. Seo, *Nature* **567**, 511 (2019).
- 19) D. H. Cao, C. C. Stoumpos, O. K. Farha, J. T. Hupp, and M. G. Kanatzidis, *J. Am. Chem. Soc.* **137**, 7843 (2015).
- 20) H. Tsai et al., *Nature* **536**, 312 (2016).
- 21) C. Ortiz-Cervantes, P. Carmona-Monroy, and D. Solis-Ibarra, *Chem. Sus. Chem* **12**, 1560 (2019).
- 22) N. Parikh, M. M. Tavakoli, M. Pandey, A. Kalam, D. Prochowicz, and P. Yadav, *Sustain. Energy Fuels* **5**, 1255 (2021).
- 23) D. H. Cao, C. C. Stoumpos, T. Yokoyama, J. L. Logsdon, T.-B. Song, O. K. Farha, M. R. Wasielewski, J. T. Hupp, and M. G. Kanatzidis, *ACS Energy Lett.* **2**, 982 (2017).
- 24) Y. Sanehira, Y. Numata, M. Ikegami, and T. Miyasaka, *Chem. Lett.* **46**, 1204 (2017).
- 25) R. Arai, M. Yoshizawa-Fujita, Y. Takeoka, and M. Rikukawa, *ACS Omega* **2**, 2333 (2017).
- 26) Y. Chen, Y. Sun, J. Peng, W. Zhang, X. Su, K. Zheng, T. Pullerits, and Z. Liang, *Adv. Energy Mater.* **7**, 1700162 (2017).
- 27) Y. Chen, Y. Sun, J. Peng, J. Tang, K. Zhen, and Z. Liang, *Adv. Mater.* **30**, 1703487 (2018).
- 28) G. Grancini and M. K. Nazeeruddin, *Nat. Rev. Mater.* **4**, 4 (2019).
- 29) A. Z. Chen, M. Shiu, J. H. Ma, M. R. Alpert, D. Zhang, B. J. Foley, D.-M. Smilgies, S.-H. Lee, and J. J. Choi, *Nat. Commun.* **9**, 1 (2018).
- 30) C. C. Stoumpos, D. H. Cao, D. J. Clark, J. Young, J. M. Rondinelli, J. I. Jang, J. T. Hupp, and M. G. Kanatzidis, *Chem. Mater.* **28**, 2852 (2016).
- 31) D. Yang, R. Yang, K. Wang, C. Wu, X. Zhu, J. Feng, X. Ren, G. Fang, S. Priya, and S. F. Liu, *Nat. Commun.* **9**, 3239 (2018).
- 32) A. Kubono and R. Akiyama, *Mol. Cryst. Liq. Cryst.* **378**, 167 (2002).
- 33) A. Kubono and R. Akiyama, *J. Appl. Phys.* **98**, 093502 (2005).